Journal of Molecular Spectroscopy 254 (2009) 39–46

Contents lists available at ScienceDirect

Journal of Molecular Spectroscopy

journal homepage: www.elsevier.com/locate/jms

High-resolution infrared spectra of the two nonpolar isomers of 1,4-difluorobutadiene

Norman C. Craig [a,*], Michael C. Moore [a], Chistopher F. Neese [a], David C. Oertel [a], Laura Pedraza [a], Tony Masiello [b]

[a] Department of Chemistry and Biochemistry, Oberlin College, 119 Woodland St., Oberlin, OH 44074, USA
[b] Environmental and Molecular Sciences Laboratory, Pacific Northwest National Laboratory, P.O. Box 999, Mail Stop K8-88, Richland, WA 99352, USA

ARTICLE INFO

Article history:
Received 3 December 2008
In revised form 6 January 2009
Available online 21 January 2009

Keywords:
1,4-Difluorobutadiene isomers
High-resolution
Infrared
Rotational analysis
Rotational constants

ABSTRACT

High-resolution (0.0013 cm^{-1}) infrared spectra have been recorded for *trans,trans*-1,4-difluorobutadiene (ttDFBD) and *cis,cis*-1,4-difluorobutadiene (ccDFBD). The rotational structure in two C-type bands (ν_{10} and ν_{12}) and one A-type band (ν_{22}) for ttDFBD and in two C-type bands (ν_{11} and ν_{12}) for ccDFBD has been analyzed. Ground state and upper state rotational constants, except for ν_{10} of ttDFBD, have been fitted. Band centers are 934.1 cm^{-1} (ν_{10}), 227.985 cm^{-1} (ν_{12}), and 1087.919 cm^{-1} (ν_{22}) for ttDFBD. Band centers are 762.891 cm^{-1} (ν_{11}) and 327.497 cm^{-1} (ν_{12}) for ccDFBD. The small inertial defects in the ground state confirm that both isomers are planar. Obtaining the ground state rotational constants for the two isomers of DFBD is a first step toward determining their semi-experimental equilibrium structures.

1. Introduction

Viehe and Franchimont were the first to prepare the three isomers of 1,4-difluorobutadiene (DFBD) and report the unusual energy relationship among them [1,2]. The *cis,cis* isomer, which has the closest approach of the fluorine atoms to the neighboring electron-rich double bonds, has the lowest energy, and the *trans,trans* isomer, which has the fluorine atoms most distant from the double bonds, has the highest energy. Using simpler chemistry to make DFBD, Craig et al. recorded the infrared and Raman spectra and assigned all the vibrational fundamentals of the three isomers [3].

To gain insight into the unusual energy relationships in the isomers of DFBD and to examine the influence of fluorine substitution on the π-electron distribution in butadiene, we have launched a program with the goal of fitting semi-experimental equilibrium structures to the three isomers of DFBD. A preliminary semi-experimental equilibrium structure of the polar *cis,trans* isomer was determined from a combination of ground state rotational constants obtained in a microwave investigation and quantum chemical calculations [4,5]. The nonpolar *trans,trans* and *cis,cis* isomers are microwave silent and must be investigated by high-resolution infrared spectroscopy. An equilibrium structure of butadiene itself, which shows the structural effects of π-electron delocalization, has recently been published [6].

This paper presents the first results of investigating the *trans,trans* and *cis,cis* isomers of DFBD by high-resolution (0.0013 cm^{-1}) infrared spectroscopy. Ground state rotational constants are reported from the analysis of the rotational structure in two C-type bands and one A-type band of the *trans,trans* isomer and in two C-type bands of the *cis,cis* isomer.

2. Experimental

Samples were synthesized by reaction of *cis*-3,4-dichlorocyclobutene (Fluka) with silver difluoride (Aldrich) to give mostly *trans*-3,4-difluorocyclobutene, which was isomerized at 100 °C with iodine catalysis to give a mixture of the three isomers of 1,4-difluorobutadiene [3]. Individual isomers were isolated by preparative gas chromatography [3]. For shipping, samples were inhibited with hydroquinone and sealed in glass ampoules.

High-resolution spectra were recorded on a Bruker IFS 125 FS spectrometer at PNNL. Samples were contained in a multi-pass White cell. Table 1 summarizes the conditions used in recording the spectra. Initial spectra of the first C-type bands of the *trans,trans* and *cis,cis* isomers were recorded with 0.0018 and 0.0021 cm^{-1} resolution, respectively, by Dr. Michael Lock on the Bruker 120 instrument at Justus Liebig Universität in Giessen, Germany.

Finding and working with subband series was greatly aided by use of Loomis–Wood pattern-recognition software [9]. A number of locally written Fortran programs also assisted in handling the

* Corresponding author. Fax: +1 440 775 6682.
E-mail address: norm.craig@oberlin.edu (N.C. Craig).

0022-2852/$ - see front matter © 2009 Elsevier Inc. All rights reserved.
doi:10.1016/j.jms.2009.01.003

Table 1
Experimental conditions for spectra.

Region/cm^{-1}	Resolution/cm^{-1}	Beam-splitter	Detector	No. of scans	Pathlength/m	Press./Torr	Calibrant gas
ttDFBD							
600–1000	0.0015	KBr	HgCdTe[a]	704	12.8	0.178	CO_2[b]
600–1100	0.0013	KBr	HgCdTe[a]	768	3.2	0.077	CO_2[b]
600–1100	0.0013	KBr	HgCdTe[a]	256	3.2	0.032	CO_2[b]
190–500	0.0013	Mylar	Si[c]	128	12.8	0.46	H_2O[d]
ccDFBD							
600–1070	0.0014	KBr	HgCdTe[a]	256	3.2	0.26	CO_2[b]
600–1000	0.0013	KBr	HgCdTe[a]	384	3.2	0.12	CO_2[b]
200–650	0.0013	Mylar	Si[c]	96	19.2	0.33	H_2O[d]
150–700	0.0013	Mylar	Si[c]	96	3.2	~0.5	H_2O[d]

[a] Liquid nitrogen temperature.
[b] Ref. [7].
[c] Bolometer; liquid helium temperature.
[d] Ref. [8].

large datasets. For fitting ground state combination differences (GSCDs) to the ground state (GS) rotational constants in a Watson-type Hamiltonian [10], a modification of Dr. Arthur Maki's ASYM program was employed. The asymmetric reduction and the I^r representation were used. Redundant use of lines from subband series with asymmetry splitting was avoided in computing GSCDs. Upper state (US) rotational constants were fitted to similar Hamiltonians with the GS constants held fixed. As needed, some quartic centrifugal distortion constants were supplied from calculations using a B3LYP/aug-cc-pVTZ model with Gaussian 03 (G03) software [11]. Cartesian coordinates were transformed into the principal axis system before use in the vibration–rotation module of G03 [12,13].

3. Results and discussion

3.1. General considerations

As shown schematically in Fig. 1, both *trans,trans*- and *cis,cis*-DFBD are near-prolate symmetric tops with C_{2h} symmetry. Twelve of their 24 normal modes are infrared active. The *a* principal rotation axis passes through the center of inversion and roughly bisects the C–F bonds. The *b*-axis also lies in the plane of the molecule. The *c* rotation axis is perpendicular to the molecular plane. Consequently, the normal modes of the b_u symmetry species, which have displacements in the molecular plane, give hybrid A/B-type band shapes in gas phase infrared spectra. Normal modes of the a_u symmetry species with displacements perpendicular to the molecular plane give C-type band shapes. Only A-type and C-type bands were investigated in this study. Selection rules for rotational transitions in A-type bands are $\Delta J = 0, \pm1$; $\Delta K_a = 0$; and $\Delta K_c = \pm1$. Selection rules for rotational transitions in C-type bands are $\Delta J = 0, \pm1$; $\Delta K_a = \pm1$; and $\Delta K_c = 0, \pm2$.

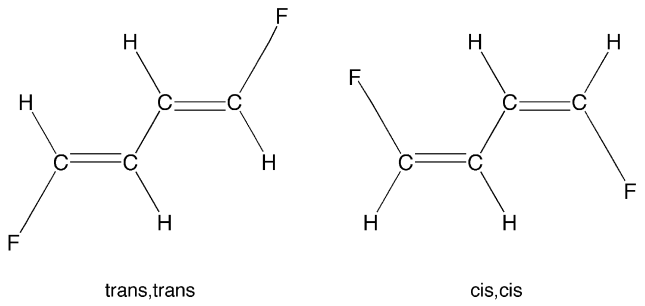

Fig. 1. Schematic structures for *trans,trans*-1,4-difluorobutadiene and *cis,cis*-1,4-difluorobutadiene.

3.2. Revised assignments of fundamentals

A reconsideration of the two lowest vibrational frequencies for the *trans,trans* isomer has led to an exchange of their assignments. Our previous assignment gave $\nu_{13}(a_u)$ the higher frequency and $\nu_{24}(b_u)$ the lower frequency, despite the predictions from quantum chemical calculations available at that time [3]. The problem in making these two assignments is the complex band shape of the gas phase infrared spectrum in the region from 170 to 130 cm^{-1} [3]. Our high-resolution infrared scan in the low frequency region did not go low enough to provide new information. In the previous assignment, the apparent Q branch at 154 cm^{-1} was decisive in making the assignments. We now prefer to assign the depression at 147 cm^{-1} as the center of a B-type band for ν_{24} and regard the structure with added intensity near 133 cm^{-1} as the overlap of the P branch of the band for ν_{24} and the Q branch for ν_{13}. Taking a frequency in the lower part of the overlapped band gives an approximate frequency for ν_{13} of 127 cm^{-1}. Not only does this revised interpretation conform to the band shapes, but it also agrees with the new predictions from the DFT calculations, which give, without any scaling, 145 cm^{-1} for ν_{24} and 124 cm^{-1} for ν_{13}. These predictions are very close to the previous Adiabatic Connection Method calculations, which gave 146 and 127 cm^{-1}, respectively [3]. The normal coordinate for ν_{24} has a substantial contribution from CF in-plane bending, and the normal coordinate for ν_{13} has a substantial amount of out-of-plane CF bending. The nearly perpendicular CF motions in these two modes are favorable for Coriolis coupling, and the direct product of these two modes has the correct symmetry species for Coriolis coupling. Such coupling could cause large perturbations in the rotational states and the intensities of the two bands, as was seen for *trans*-1,2-difluoroethylene, which is a similar case [14].

We also note a typographical error in one fundamental frequency reported for the *cis,cis* isomer of DFBD [3]. The frequency for ν_{16} observed in the liquid-phase Raman spectrum should be 560 cm^{-1} instead of 580 cm^{-1}. We discovered this error by its effect on the interpretation of a Fermi resonance. Two similar bands of the same intensity occur at 644 and 620 cm^{-1} in the gas phase infrared spectrum of ccDFBD. The fundamental for $\nu_{23}(b_u)$ is expected in this region. The correction for ν_{16} gives 638 cm^{-1} for the estimate of the $\nu_{13} + \nu_{16}$ combination tone, as was correctly reported [3] and as would be reasonable for Fermi resonance between the combination state of B_u symmetry and the $\nu_{23}(b_u)$ fundamental. The absence of any Q-branch features in either band in the high-resolution infrared spectrum confirms that both bands

are for transitions of the B_u symmetry species, thereby supporting the previous interpretation of Fermi resonance.

3.3. Analysis of high-resolution spectra of trans,trans-1,4-difluorobutadiene

3.3.1. C-type band centered at 934 cm^{-1}

The vibrational transition at 934 cm^{-1}, assigned to $\nu_{10}(a_u)$ of ttDFBD [3], is caused by out-of-plane flapping of C–H bonds with a greater contribution of the interior hydrogen atoms. An overall view of this C-type band is presented in Fig. 2. We analyzed this rather intense spectrum, which is far from being baseline resolved, to provide access to high-K_a subbands. Although the overall appearance of this band suggests its rotational structure is assignable, evidence of perturbations is immediately apparent. The intensity of the Q branches for subbands drops very low and the spacing becomes anomalous in the $K_a' = 11$ region. Q branches for subbands vary in intensity, and the spacing between these Q branches is unsystematic in other parts of the band. Q branch features are unmarked for $^{P}Q_{17}$, $^{P}Q_{12}$, $^{R}Q_{10}$, and $^{R}Q_{15}$ because match-ups between possible subband series could not be confirmed with $^{R}R_{15}/^{P}P_{17}$ and $^{R}R_{10}/^{P}P_{12}$ GSCDs, predicted while fitting observed GSCDs to GS rotational constants.

A perturbation near the band center interfered with attempts to predict assignments for subbands below $K_a'' = 3$ in the R branch and below $K_a'' = 5$ in the P branch. A less intense scan of the spectrum did not help in assigning subband series near the band center. For this near-prolate top ($\kappa = -0.997$, information in this band about the difference between the B and C rotational constants for the GS came principally from the weak dependence of the difference between B and C difference in subbands without observable asymmetry splitting at higher K_a [15]. For improved information about the B and C rotational constants, it was desirable to analyze the rotational structure in at least one other band, as was done.

Most of the assignment of the 934 cm^{-1} band was drawn from the spectrum recorded at PNNL. However, this spectrum was too noisy to be useful above 985 cm^{-1} because the high-end filter had been set too low. To extend the subband series to $^{R}R_{29}$, we used assignments for subbands from $^{R}R_{23}$ to $^{R}R_{29}$ made in a spectrum recorded with (0.0018 cm^{-1} resolution) at Justus Liebig Universität in Giessen, Germany. Frequencies from the Giessen spectrum were adjusted by a factor constructed from comparing wavenumbers of lines in the $^{R}R_{19}$, $^{R}R_{20}$, and $^{R}R_{22}$ subbands as observed in the two spectra.

We were unable to fit US rotational constants to assigned lines well enough (SD < 0.02 cm^{-1}) to make useful predictions of unassigned series in the 934 cm^{-1} band, even when the dataset was truncated to a few subbands toward the interior of the band. We were, however, able to assign a large number of subbands. Fig. 3 is an example of detail of the assignments in the R branch, in this case, in the vicinity of $^{R}Q_7$ and $^{R}Q_8$. Although the lines for $^{R}R_6$ look coincident with lines from $^{R}R_5$ in Fig. 3, they have different wavenumber values. Subbands were assigned in the P branch from $K_a'' = 5$ to 31 except for $K_a'' = 12$, 17 and in the R branch from $K_a'' = 3$ to 29 except for $K_a'' = 10$, 15. Tentative assignments were made for the $^{R}Q_0$ and $^{P}Q_1$ subbands. However, these assignments in the center of the band could not be checked with ground state combination differences (GSCDs). All other subband assignments were confirmed with GSCDs. A total of 1321 GSCDs was obtained from this band. An estimate of the overall band center at 934.1 cm^{-1} came from averaging estimates of the band centers of the $^{R}Q_0$ and $^{P}Q_1$ subbands. This value was supported by a rough fit of lines from the interior of the band to a Hamiltonian.

After consideration of the analysis of the second C-type band of the *trans,trans* isomer, we present the results of fitting GS rotational constants to the combined GSCDs for the three bands. The GSCDs from the band at 934 cm^{-1} are part of the Supplementary data for all three bands. Supplementary Table S1 contains the lines assigned for the band centered at 934 cm^{-1}.

3.3.2. C-type band centered at 228 cm^{-1}

The vibrational transition at 228 cm^{-1} arises from $\nu_{12}(a_u)$ for ttDFBD [3]. This normal coordinate involves some out-of-plane movement of the end carbon atoms as well as the two sets of hydrogen atoms. At first glance the overall appearance of the C-type band for ν_{12} shown in absorbance in Fig. 4 gives little promise for analysis of the rotational structure. Strong lines from residual water in the spectrometer dominate the spectrum. The recorded band is weak, and the S/N looks too low. One helpful feature is that the Q branches of subbands are quite sharp because A' differs little from A''. The prominence of Q branches permitted assigning Q branches for two hot bands in addition to the Q branches of the fundamental. Table 2 gives the assignments for the Q branches in the two hot bands, which were fitted to quadratic polynomials [16]. Parameters of the two fits are included at the bottom of the table. The band centers for the hot bands are 225.161 and 222.526 cm^{-1}. We presume that thermal excitation of $\nu_{13}(a_u)$ causes the hot bands. The low frequency of ν_{13} gives sufficient thermal excitation at room temperature to account for the inten-

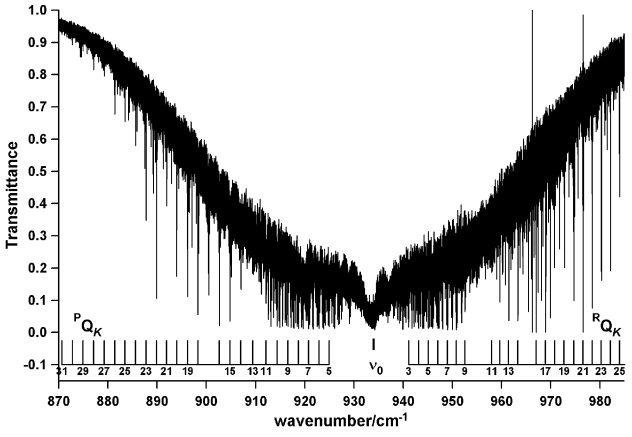

Fig. 2. Overall appearance of the C-type band of *trans,trans*-1,4-difluorobutadiene centered a 934 cm^{-1} showing combs for $^{P}Q_K$ and $^{R}Q_K$ subbands (0.18 Torr, 2.3 m Torr).

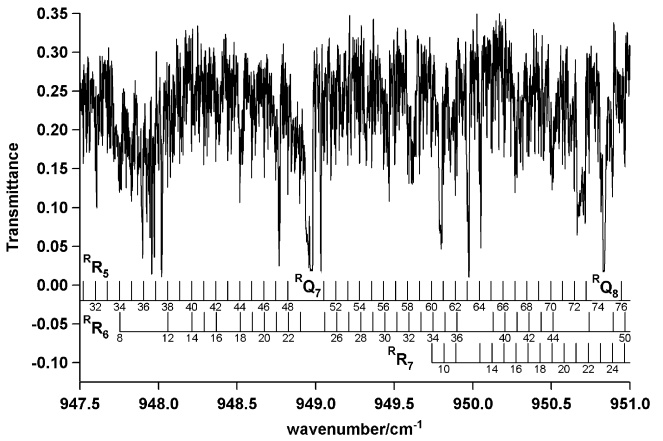

Fig. 3. Detail of assignments of $^{R}R_K$ subbands for ttDFBD near $^{R}Q_7$ and $^{R}Q_8$ in the band at 934 cm^{-1}.

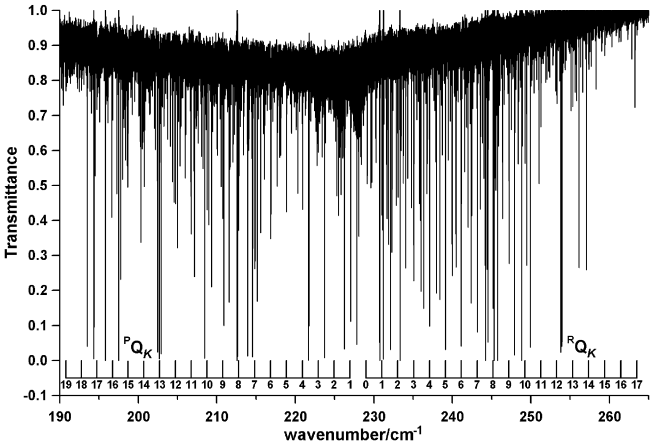

Fig. 4. Overall appearance of the C-type band of *trans*,*trans*-1,4-difluorobutadiene centered a 228 cm^{-1} showing combs for $^{P}Q_K$ and $^{R}Q_K$ subbands and hot bands centered at 225.161 and 222.526 cm^{-1} (0.46 Torr, 5.9 m Torr). Most of the strong lines are from water in the spectrometer.

Table 2
Q branches of the first and second hot bands of the C-type band for *trans*,*trans*-1,4-difluorobutadiene at 228 cm^{-1} and their fit to polynomials (in cm^{-1}).

K_a	ν_Q (hot 1)	Obs–calc (hot 1)	ν_Q (hot 2)	Obs–calc (hot 2)
−15	196.155	0.021		
−14	198.120	0.007		
−13	200.093	−0.004		
−12	202.075	−0.008		
−11	204.062	−0.010	201.441	0.015
−10	206.054	−0. 011	203.460	0.040
−9	208.052	−0.010	205.438	0.021
−8	210.054	−0.007	207.421	0.003
−7	212.060	−0.004	209.412	−0.010
−6	214.070	0.000	211.405	−0.024
−5	216.082	0.003	213.408	−0.031
−4	218.098	0.006	215.41	−0.043
−3	220.116	0.008	217.429	−0.041
2	230.247	0.011		
3	232.277	0.005	229.623	−0.015
4	234.315	0.004	231.675	−0.002
5	236.352	−0.001	233.731	0.012
6	238.395	−0.003	235.802	0.037
7	240.444	−0.003	237.874	0.060
8	242.499	0.000	239.868	0.002
9	244.559	0.005	241.979	0.058
10	246.613	0.001	244.006	0.026
11	248.668	−0.006	246.024	−0.018
12	250.728	−0.001	248.069	−0.038
13	252.804	−0.004	250.123	−0.052
14	254.889	0.010		
Parameters in cm^{-1}				
ν_0	225.161(3)		222.525(14)	
$A' - B'$	1.0137(1)		1.014(1)	
$\Delta A - \Delta B$	0.00164(2)		0.0016(2)	

sity of the hot bands, and coupling between two modes of the a_u symmetry species is likely to be favored.

The combs in Fig. 4 indicate that Q branches have been assigned for ν_{12} from $^{P}Q_{19}$ to $^{R}Q_{17}$. With the exception of $^{P}P_1$ and $^{R}R_0$, subband series from $^{P}P_{19}$ to $^{R}R_{17}$ were assigned. In addition, $^{P}Q_1$ and $^{R}Q_0$ were assigned. In contrast to the analysis of the C-type band at 934 cm^{-1}, the analysis of the band center of the C-type band at 228 cm^{-1} gave valuable information about the difference between the *B* and *C* rotational constants from asymmetry splitting. Fig. 5 shows details of the assignment of $^{P}P_5$, $^{P}P_6$, and $^{P}P_7$ subbands in the vicinity of $^{P}Q_6$ and $^{P}Q_7$. $^{P}P_5$ begins to show asymmetry splitting at $J = 57$, but the effect is barely discernible within the wavenumber range of Fig. 5. Q branches for hot band series are seen in Fig. 5.

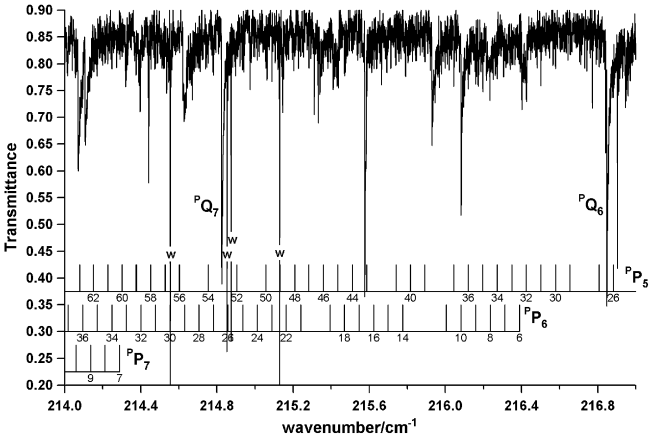

Fig. 5. Detail of assignments of $^{P}P_K$ subbands for ttDFBD near $^{P}Q_6$ and $^{P}Q_7$ in the band at 228 cm^{-1}. Four lines from water are marked with "w".

Table 3
Rotational constants for the ground state and two upper states of *trans*,*trans*-1,4-difluorobutadiene.

	GS[a,b]	ν_{12}[a]	ν_{22}[a]
A (cm^{-1})	1.0507501(4)	1.0506038(4)	1.051265(2)
B (cm^{-1})	0.0389695(1)	0.03896426(4)	0.0389145(1)
C (cm^{-1})	0.0375821(1)	0.03759105(3)	0.0375223(1)
Δ[c] (amu Å^2)	−0.07395	−0.24111	0.03766
$\delta_J \times 10^{10}$ (cm^{-1})	0.59298[d]	0.73(3)	0.79(9)
$\delta_K \times 10^{8}$ (cm^{-1})	0.71240[d]	0.71240[d]	0.71240[d]
$\Delta_K \times 10^{6}$ (cm^{-1})	3.9266(3)	2.014(2)	2.96(3)
$\Delta_{JK} \times 10^{8}$ (cm^{-1})	−3.7388(7)	−4.307(5)	−3.75(2)
$\Delta_J \times 10^{9}$ (cm^{-1})	1.327(10)	1.328(1)	1.316(2)
ν_0 (cm^{-1})		227.98468(2)	1087.91920(2)
$\Delta\nu_{rms}$ (cm^{-1})	0.000352	0.000309	0.000326
κ	−0.997261	−0.997289	−0.997253
No. of *trans*.	2813	2130	1293
Max. K_a'	30[e], 18[f], 9[g]	14	8
Max. J	90[e], 90[f], 83[g]	98	96

[a] Uncertainty (1σ) in the last places in the fit is in parentheses.
[b] Fit to GSCDs from ν_{10} (1321), ν_{12} (960), and ν_{22} (532).
[c] Inertial defect $\Delta = I_c - I_a - I_b$.
[d] Computed with Gaussian 03 and the B3LYP/aug-cc-pVTZ model.
[e] For ν_{10}.
[f] For ν_{12}.
[g] For ν_{22}.

The results of fitting GS rotational constants to GSCDs and then fitting US rotational constants to information from transitions are presented in Table 3. The 2813 GSCDs used in the fitting of GS rotational constants are a composite of those from the 934 cm^{-1} band (1321), from the 228 cm^{-1} band (960), and from the 1088 cm^{-1} A-type band (532), yet to be discussed. For the GS rotational constants, attempts to fit δ_J and δ_K gave uncertainties comparable to the values of the parameters. Consequently, GSCDs were fitted using fixed values for δ_J and δ_K predicted from a G03 calculation with a B3LYP/aug-cc-pVTZ model [12–14]. Supporting the use of the calculated values for δ_J and δ_K was the agreement within 3.2% between calculated Δ_K, Δ_{JK}, and Δ_J and their observed values. The small value of −0.07395 amu Å^2 for the inertial defect of the GS of ttDFBD (Table 3) confirms the planarity of this molecule. In fitting the US rotational constants, only δ_K was constrained to the theoretical value. Included in Table 3 are the US rotational constants for ν_{12} obtained from fitting series from $^{P}P_{15}$ to $^{R}R_{13}$. A perturbation apparent at $K_a' = 15$ limited the fit to subband series with lower K_a' values. A total of 2130 lines were used in the fit for the US

rotational constants; 391 additional lines were assigned in the perturbed region. The band center for ν_{12} is 227.985 cm^{-1}.

The GSCDs for all three bands analyzed and the fitting of these GSCDs to GS constants are supplied in Supplementary Table S2. In this table the GSCDs for ν_{10} are first; the GSCDs for ν_{12} are second. The lines from the 228 cm^{-1} band fitted to the US rotational constants along with the details of the fit are in Supplementary Table S3.

3.3.3. A-type band centered at 1088 cm^{-1}

The third band in the high-resolution infrared spectrum of ttDFBD to be analyzed was the intense A-type band centered at 1088 cm^{-1}. This transition is for $\nu_{22}(b_u)$, which has a significant component of antisymmetic CF stretching along the *a* rotation axis and an admixture of antisymmetric CH bending. Fig. 6 shows the overall structure of the band. The narrow Q branch for the fundamental, which is supplemented with weaker Q branches for hot bands degrading to lower frequency, makes the analysis of this band reasonably straightforward. The lack of a perturbation below $K_a = 9$ also simplified the analysis because lines for subbands with low values of K_a could be predicted as the first step in their assignment. Fig. 6 is of a low intensity scan (0.032 torr, 0.10 m Torr). The rotational analysis was done on a medium intensity scan (0.077 Torr, 0.25 m Torr).

Subbands extending from the R branch through the band center to the P branch were assigned for $K_a = 0$–9. At the start of the assignment, A-type GSCDs provided links between $^{Q}P_K$ and $^{Q}R_K$ series. The GSCDs were predicted while fitting GS rotational constants to GSCDs from the two C-type bands. All of the assignments of subbands for the A-type band are shown in the Loomis–Wood display in Fig. 7.

GSCDs from the A-type band were joined with those from the two C-type bands in a single fitting. The GS rotational constants obtained from the pooled data are given in column one in Table 3. An attempt to fit the GSCDs from the A-type band alone gave unacceptable results because the data for a band with a single tight central Q branch gives a poor definition of the *A* rotational constant. However, asymmetry splitting from the interior of the A-type band helped define the difference between *B* and *C* in the fit of the GS rotational constants. The narrow central Q branch is a consequence of the small difference between the A'' and A' rotational constants.

Table 3 contains US rotational constants for ν_{22}. Because of the onset of a perturbation, the lines for $K_a = 9$ (138 lines) were omitted from this fit of 1293 lines. Even though the fit of the GS rotational constants alone for this A-type band was unacceptable, the fit of the US rotational constants with the GS rotational constants held fixed was acceptable, as reported in Table 3. Fixing the GS rotational constants made possible the fit to the upper state rotational constants. δ_K was also held at the GS value. The band center is 1087.919 cm^{-1}. Supplementary Table S4 gives the lines assigned for ν_{22} and the results of fitting them to US rotational constants.

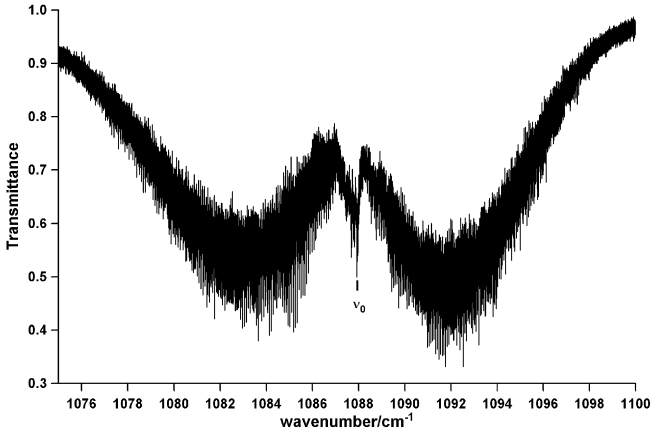

Fig. 6. Overall appearance of the A-type band of *trans*,*trans*-1,4-difluorobutadiene at 1088 cm^{-1} (0.032 Torr, 0.10 m Torr).

3.4. cis,cis-1,4-Difluorobutadiene

3.4.1. C-type band centered at 763 cm^{-1}

The overall structure of the C-type band for *cis*,*cis*-DFBD centered at 763 cm^{-1} is displayed in Fig. 8, the highest intensity scan. This band is for $\nu_{11}(a_u)$, which is nearly equal parts out-of-plane flapping of the two kinds of hydrogen atoms. The combs for the Q branches assigned to subbands extend from $K_a'' = 4$ to 32 in the P branch and from $K_a'' = 3$ to 30 in the R branch. Fig. 9 shows some of the detail in the assignments for the beginnings of the $^{P}P_7$, $^{P}P_8$, and $^{P}P_9$ subbands. In addition to the Q branches for $K_a'' = 8$–11, Q branches for hot bands are apparent in this figure.

Numerous hot bands contribute to the complex band center, as shown in detail in Fig. 10. At least two hot band series, degrading to low frequency, can be identified. One sequence has a wider spacing of approximately 0.76 cm^{-1}; the other series has a narrower spacing of approximately 0.1 cm^{-1}. A third hot band series with a spacing of approximately 0.51 cm^{-1} might be present. Good candidates for hot bands are thermal excitation of $\nu_{13}(a_u)$ at 78 cm^{-1} and $\nu_{24}(b_u)$ at 165 cm^{-1}. Although the rate of intensity decrease could, in principle, distinguish between the originating vibrations, the structure of the band center is too complex for intensities to be a useful guide. Because coupling between the out-of-plane ν_{11} mode and the out-of-plane ν_{13} mode is likely to be strong, the hot bands with the wider separation probably arise from this interaction. A third hot band series might arise from thermal excitation of $\nu_9(a_g)$ at 232 cm^{-1}. Attempts to carry the assignment of $^{R}R_K$ inside $K_a'' = 3$ and $^{P}P_K$ inside $K_a'' = 4$ failed because of the extent of hot band Q branches in the band center. We attempted to jump over the gap in assignments of $^{R}R_K$ and $^{P}P_K$ subbands near the band center and assign the $^{P}Q_1$ and $^{R}Q_0$ subbands that form the central Q branch. Because the spacing of lines in this region is very tight, predictions made while fitting US rotational constants did not lead to unambiguous assignments. We abandoned the attempt to assign the central Q branch.

Assignments of some of the subbands for this first C-type band proved dubious through comparisons of GSCDs after the analysis of the second C-type band centered at 327.5 cm^{-1}, which is discussed below. A cause of the misassignments in the first C-type band was the entanglement of $^{P}P_K$ series in the $K_a = 13$–19 range. The extent of this problem is shown in the LW display in Supplementary Fig. S1.

Table 4 contains the rotational constants fitted to the rotational transitions assigned in the band for ν_{11}. The GS constants were fitted to the pooled GSCDs derived from the analysis of the C-type band for ν_{12} as well as those obtained from the band for ν_{11}. In total, 2014 GSCDs were used in fitting the GS constants. The dataset was not sufficiently robust to give an acceptable fit to δ_J and δ_K as well as the other three quartic centrifugal distortion constants. Values for these two quartic centrifugal distortion constants were taken from the G03 calculations for ccDFBD performed with a B3LYP/aug-cc-pVTZ model [11]. Agreement between the three Δ centrifugal distortion constants, which were fitted, and the predicted ones was within 4.2%, thereby justifying the use of predicted values for δ_J and δ_K. The small value of −0.08848 amu $Å^2$ for the inertial defect of the GS confirms that ccDFBD is a planar molecule. For the GS of ccDFBD, κ is −0.971 in comparison with $\kappa = -0.997$ for ttDFBD. Thus, ccDFBD is somewhat further from a prolate symmetric top than ttDFBD.

Table 4 also contains the US rotational constants fitted to assigned lines while holding the GS rotational constants fixed. A to-

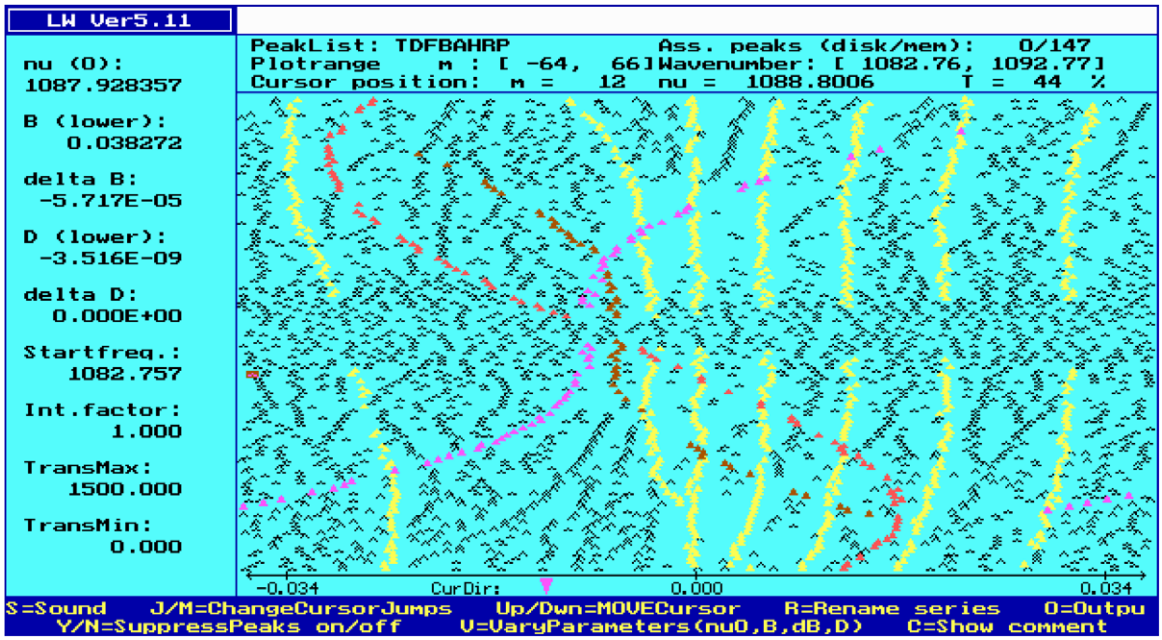

Fig. 7. A Loomis–Wood display of the assignments of subbands of ttDFBD in the A-type band (0.077 Torr, 0.25 m Torr). Yellow series (left to right) are for K_a = 9, 3–8. Violet for 0, red for 1, and orange for 2. (For interpretation of the references to colour in this figure legend, the reader is referred to the web version of this article.)

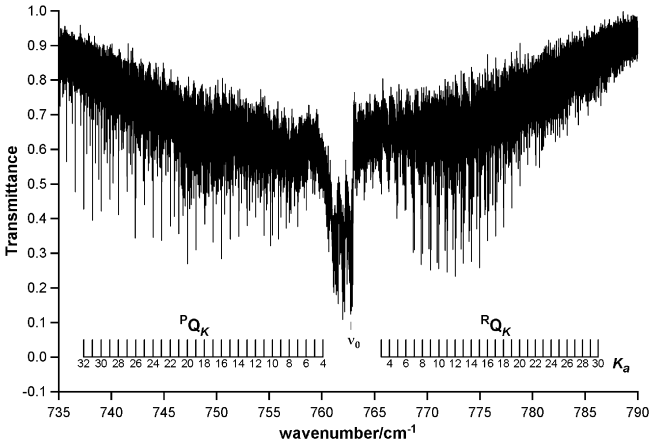

Fig. 8. Overall appearance of the C-type band of *cis,cis*-1,4-difluorobutadiene centered at 763 cm^{-1} showing combs for $^{P}Q_K$ and $^{R}Q_K$ subbands (0.26 Torr, 0.83 m Torr).

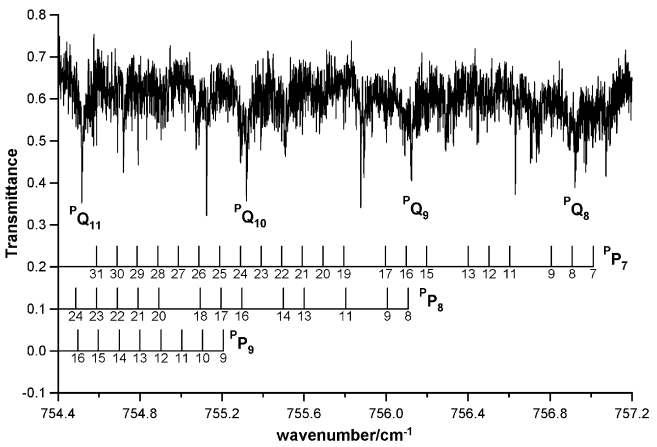

Fig. 9. Detail of assignments of $^{P}P_K$ subbands of ccDFBD near $^{P}Q_8$ to $^{P}Q_{11}$ in the band at 763 cm^{-1}.

tal of 2103 lines with K_a' reaching 31 were used in the US fitting for ν_{11}. The same calculated values for δ_J and δ_K that were part of the GS fit were adopted for the US fit. The close agreement of the three Δ centrifugal distortion constants for the GS and US supports using the same values for δ_J and δ_K in the GS and US fits. The band center is 762.891 cm^{-1}. Supplementary Table S5 contains the GSCDs for ν_{11} and for ν_{12}, which will be discussed below, and the details of the fit. The GSCDs for ν_{11} come first in this table. Supplementary Table S6 contains comparable information for the US fit for ν_{11}.

3.4.2. C-type band centered at 327.5 cm^{-1}

Our practice has been to analyze the rotational structure in a second band of a molecule to confirm the analysis of the first band. The merit in this practice was affirmed for ccDFBD when we found that the GSCDs from the second band disagreed somewhat from those for the first band and traced the errors to misassignments in the first band.

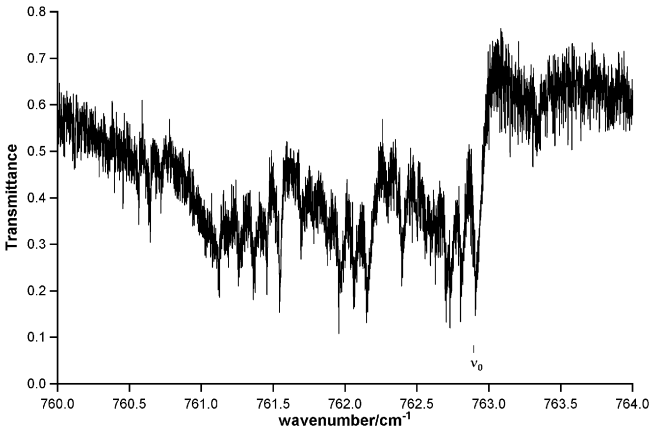

Fig. 10. Multiple Q branches from hot bands in the center of the C-type band at 793 cm^{-1} for ccDFBD.

Table 4
Rotational constants for the ground state and two upper states of *cis*,*cis*-1,4-difluorobutadiene.

	Ground state[a,b]	v_{11}[a]	v_{12}[a]
A (cm^{-1})	0.4465210(5)	0.4458257(1)	0.4452894(1)
B (cm^{-1})	0.053655(1)	0.0536536(3)	0.0537033(5)
C (cm^{-1})	0.0479110(7)	0.0479217(4)	0.0479448(5)
Δ[c] (amu Å^2)	−0.08848	−0.23149	−0.15529
$\delta J \times 10^8$ (cm^{-1})	0.10848[d]	0.10848[d]	0.10848[d]
$\delta_K \times 10^7$ (cm^{-1})	0.22351[d]	0.22351[d]	0.22351[d]
$\Delta_K \times 10^7$ (cm^{-1})	7.711(5)	7.703(1)	6.707(2)
$\Delta_{JK} \times 10^8$ (cm^{-1})	−9.23(3)	−9.218(4)	−9.721(4)
$\Delta_J \times 10^9$ (cm^{-1})	7.86(6)	7.869(4)	7.958(4)
v_0 (cm^{-1})		762.89060(2)	327.49682(3)
Δv_{rms} (cm^{-1})	0.00035	0.00031	0.00036
κ	−0.97118	−0.97119	−0.97101
No. of lines	2014	2103	2286
Max. K_a'	32[e], 33[f]	31	30
Max. J	71[e], 77[f]	71	78

[a] Uncertainty in last decimal place in parentheses.
[b] Fit to pooled GSCDs from the bands for v_{11} (866) and v_{12} (1148).
[c] Inertial defect $\Delta = I_c - I_a - I_b$.
[d] From the G03 calculation with the B3LYP/aug-cc-pVTZ model.
[e] For v_{11}.
[f] For v_{12}.

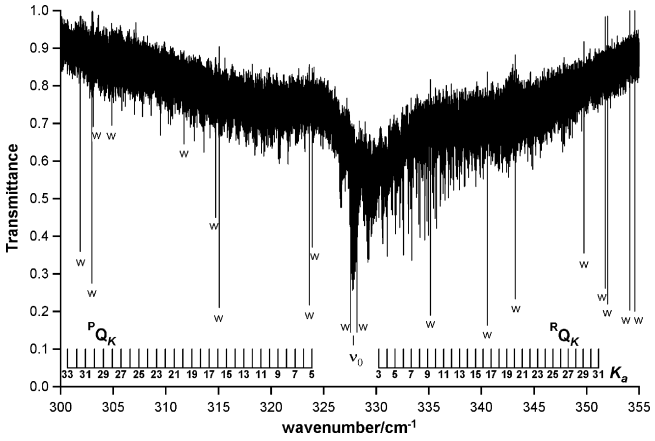

Fig. 11. Overall appearance of the C-type band of *cis*,*cis*-1,4-difluorobutadiene centered at 327.5 cm^{-1} showing combs for ^PQ_K and ^RQ_K subbands (0.33 Torr, 6.3 m Torr).

The second band to be analyzed for ccDFBD was the C-type band centered at 327.5 cm^{-1}. This band arises from the $v_{12}(a_u)$ vibrational transition, which is largely flapping of the end hydrogen atoms with components of out-of-plane motion from the two sets of carbon atoms. The overall appearance of this band is shown in Fig. 11. With only one exception, hot band centers degrade to high frequency. The intensity of the band displayed in Fig. 11 (~1.7 m Torr) is weaker than for the band that was analyzed (6.3 m Torr). The figure includes combs marking the Q branches of the subbands that were assigned. Strong sharp features marked with "w" are from water. The spread of hot band centers interfered with carrying subband assignments all the way to the band center. Subbands were assigned for $K_a'' = 5$–33 in the P branch and $K_a'' = 3$–31 in the R branch. Fig. 12 shows the details of assignments for $^RR_4$, $^RR_5$ and the beginning of $^RR_6$. $^RR_4$ is beginning to show asymmetry splitting at the end of the segment. Q branches for $K_a = 5$–7 are also in this figure. An attempt was made to assign the $^PQ_1$ and $^RQ_0$ subbands in the band center, but the results were not convincing. A total of 2465 transitions, including those not used in fitting the US rotational constants, were assigned for the C-type band for v_{12} at 327.5 cm^{-1}, from which 1148 GSCDs were derived.

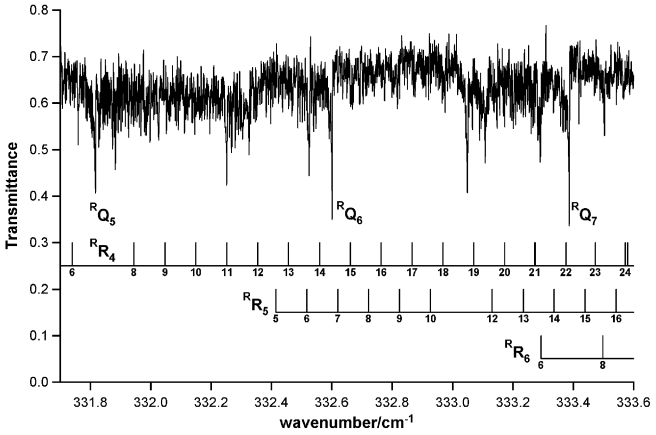

Fig. 12. Detail of assignments of ^RR_K subbands for ccDFBD near $^RQ_5$ to $^RR_7$ in the band at 327.5 cm^{-1} (~0.5 Torr, ~1.7 m Torr).

The GSCDs for the v_{12} band were combined with 866 GSCDs from the C-type band for v_{11} at 793 cm^{-1} for fitting GS rotational constants, which are reported in Table 4. US rotational constants were fitted to the transitions through $K_a' = 30$ with GS rotational constants held fixed. A small perturbation occurs at $K_a' = 31$. The US rotational constants for v_{12} are also in Table 4. For the fitting of both the GS rotational constants and the US rotational constants, δ_J and δ_K were held fixed at the values computed by G03 with the B3LYP/aug-cc-pVTZ model. The band center of 327.497 cm^{-1} reported for v_{12} is lower than the previous estimate of 330 cm^{-1}, which was a consequence of misinterpreting the broad Q branch in the band center [3]. Supplementary Table S7 gives the lines and the details of the fit of the US rotational constants.

4. Conclusions

The rotational structure in two C-type bands and one A-type band of the high-resolution infrared spectrum of ttDFBD has been assigned. GS rotational constants were fitted to the combined GSCDs from the three bands. ttDFBD is very close to being a prolate symmetric top with $\kappa = -0.997$ for the GS. The small inertial defect for the GS confirms that this molecule is planar. US rotational constants were fitted for the C-type band at 228 cm^{-1} and the A-type band at 1088 cm^{-1}. A perturbation near the band center for the C-type band near 934 cm^{-1} prevented fitting US rotational constants for this band.

The rotational structure in two C-type bands of the high-resolution infrared spectrum of ccDFBD has been assigned. One band is centered at 763 cm^{-1}; the other at 327.5 cm^{-1}. GS rotational constants were fitted to the combined GSCDs for the two bands, and US rotational constants were fitted for each band. The small inertial defect for the GS of ccDFBD confirms it as a planar molecule. The *cis*,*cis* isomer with $\kappa = -0.971$ is somewhat more asymmetric than the *trans*,*trans* isomer with $\kappa = -0.997$.

The density of lines caused by the large B and C rotational constants of ttDFBD and ccDFBD and the width of lines caused by Doppler broadening placed this study close to the edge of feasibility even with a resolution of 0.0013 cm^{-1}. Successful analysis of the rotational structure in the high-resolution infrared spectra of both the *trans*,*trans* and *cis*,*cis* isomers of DFBD has demonstrated that comparable analyses of the high-resolution spectra of lightly substituted ^{13}C and ^2H isotopomers will be possible. By adapting the synthetic strategy of Viehe and Franchimont [2], progress has been made synthesizing DFBD with selective substitution of isotopes.

Acknowledgments

We are grateful to Dr. Michael Lock, who recorded the initial high-resolution spectra of ttDFBD and ccDFBD at Justus Liebig Universität in Giessen, Germany. Deacon J. Nemchick assisted in the analysis of the bands for ttDFBD. The initial part of the investigation of the ttDFBD isomer was supported by NSF CHE-9710375. Most of the work was done under a Dreyfus Senior Scholar Mentor grant. National Science Foundation Grant 0420717 underwrote the purchase and technical support for the Beowulf computer cluster at Oberlin College. This research was also supported, in part, by the United States Department of Energy, Office of Basic Energy Sciences, Chemical Sciences Division. The high-resolution spectroscopy was performed at the W.R. Wiley Environmental Molecular Science Laboratory, a national scientific user facility sponsored by the Department of Energy's Office of Biological and Environmental Research located at the Pacific Northwest National Laboratory. Pacific Northwest National Laboratory is operated for the United States Department of Energy by Battelle under contract DE-AC05-76RLO 1830.

Appendix A. Supplementary data

Supplementary data for this article are available on ScienceDirect (www.sciencedirect.com) and as part of the Ohio State University Molecular Spectroscopy Archives (http://library.osu.edu/sites/msa/jmsa_hp.htm). Also follow style instructions from previous Word version of style sheet.

References

[1] H.-G. Viehe, Angew. Chem. Int. Ed. 2 (1963) 622.
[2] H.-G. Viehe, E. Franchimont, Chem. Ber. 97 (1964) 602–609.
[3] N.C. Craig, C.F. Neese, T.N. Nguyen, C.M. Oetel, L. Pedraza, A.M. Chaka, J. Phys. Chem. A 103 (1999) 6726–6739.
[4] N.C. Craig, C.M. Oertel, D.C. Oertel, M.J. Tubergen, R.J. Lavrich, A.M. Chaka, J. Phys. Chem. A 106 (2002) 4230–4235.
[5] N.C. Craig, P. Groner, D.C. McKean, M.J. Tubergen, Int. J. Quant. Chem. 95 (2003) 837–852.
[6] N.C. Craig, P. Groner, D.C. McKean, J. Phys. Chem. A 110 (2006) 7461–7469.
[7] L.S. Rothman, C.P. Rinsland, A. Goldman, S.T. Massie, D.P. Edwards, J.M. Flaud, A. Perrin, C. Camy-Peyret, V. Dana, J.Y. Mandin, J. Schroeder, A. McCann, R.R. Gamache, R.B. Wattson, K. Yoshino, K.V. Chance, K.W. Jucks, L.R. Brown. V. Nemtchinov, P. Varanasi, The HITRAN molecular spectroscopic database and HAWKS (HITRAN atmospheric workstation), 1996 ed., JQSRT 60 (1998) 665–710.
[8] R.A. Toth, J. Mol. Spectrosc. 190 (1998) 379–396.
[9] B.P. Winnewisser, J. Reinstädtler, K.M.T. Yamada, J. Mol. Spectrosc. 136 (1989) 12–16.
[10] N.C. Craig, O.P. Abiog, B. Hu, S.C. Stone, W.J. Lafferty, L.-H. Xu, J. Phys. Chem. 100 (1996) 5310–5317.
[11] M.J. Frisch, G.W. Trucks, H.B. Schlegel, G.E. Scuseria, M.A. Robb, J.R. Cheeseman, J.A. Montgomery Jr., T. Vreven, K.N. Kudin, J.C. Burant, J.M. Millam, S.S. Iyengar, J. Tomasi, V. Barone, B. Mennucci, M. Cossi, G. Scalmani, N. Rega, G.A. Petersson, H. Nakatsuji, M. Hada, M. Ehara, K. Toyota, R. Fukuda, J. Hasegawa, M. Ishida, T. Nakajima, Y. Honda, O. Kitao, H. Nakai, M. Klene, X. Li, J.E. Knox, H.P. Hratchian, J.B. Cross, C. Adamo, J. Jaramillo, R. Gomperts, R.E. Stratmann, O. Yazyev, A.J. Austin, R. Cammi, C. Pomelli, J.W. Ochterski, P.Y. Ayala, K. Morokuma, G.A. Voth, P. Salvador, J.J. Dannenberg, V.G. Zakrzewski, S. Dapprich, A.D. Daniels, M.C. Strain, O. Farkas, D.K. Malick, A.D. Rabuck, K. Raghavachari, J.B. Foresman, J.V. Ortiz, Q. Cui, A.G. Baboul, S. Clifford, J. Cioslowski, B.B. Stefanov, G. Liu, A. Liashenko, P. Piskorz, I. Komaromi, R.L. Martin, D.J. Fox, T. Keith, M.A. Al-Laham, C.Y. Peng, A. Nanayakkara, M. Challacombe, P.M.W. Gill, B. Johnson, W. Chen, M.W. Wong, C. Gonzalez, J.A. Pople, Gaussian, Inc., Gaussian 03, Revision C.02, Wallingford, CT, 2004.
[12] The Cartesian coordinates produced in the energy optimization were transformed to the principal rotation axis system before computing the centrifugal distortion constants. See Ref. [13].
[13] D.C. McKean, N.C. Craig, M.M. Law, J. Phys. Chem. A 112 (2008) 6760–6771.
[14] N.C. Craig, J. Overend, J. Chem. Phys. 51 (1969) 1127–1142.
[15] S.R. Polo, Can. J. Phys. 35 (1957) 880–885.
[16] J.M. Hollas, High Resolution Spectroscopy, second ed., John Wiley and Sons, Chichester, 1998.